2009 American Control Conference
Hyatt Regency Riverfront, St. Louis, MO, USA
June 10-12, 2009

$\mathcal{L}_1$ Adaptive Controller for Air-Breathing Hypersonic Vehicle with Flexible Body Dynamics

Yu Lei, Chengyu Cao, Eugene Cliff, Naira Hovakimyan, Andrew Kurdila, Kevin Wise

Abstract— **This paper presents a modified nonlinear longitudinal model for an air-breathing hypersonic vehicle and the design of an $\mathcal{L}_1$ adaptive controller for it. It is assumed that the mid-fuselage is a rigid-body, while the aft-fuselage is linearly elastic, and a rigid all-movable elevator is fixed at the end of the aft-fuselage. In the resulting mathematical model, the pitching moment depends not only on the control surface position, but also on the rate and acceleration of the control surface motion. For compensation of the modeling uncertainties including the flexible dynamics, the $\mathcal{L}_1$ adaptive control architecture is considered in this paper. It has a low-pass filter in the feedback loop allowing for arbitrarily fast adaptation with guaranteed robustness and transient performance for system's input and output signals. Simulation results demonstrate the benefits of the method.**

I. Introduction

The successful test of NASA's X-43A in 2004 affirms that air-breathing hypersonic vehicles have the potential to provide economical high-speed transportation and delivery in the future. Unlike the conventional rockets, which are powered by mixing fuel with oxygen, air-breathing hypersonic vehicles need only to carry fuel and can thus have more room for payload. However there are still numerous challenges before such vehicles can undertake commercial or military tasks.

The key challenge for design of a control system for a hypersonic vehicle is related to its peculiar structure and operational conditions. Since hypersonic vehicles tend to have slender and lightweight structure, they vibrate when operating at a very high speed. Furthermore, unlike conventional aircraft, the airframe of the air-breathing hypersonic vehicle is designed to be highly integrated with the supersonic combustion ramjet (scramjet). Additionally, the vehicle's slenderness and its lightweight fuselage cause bending and vibration, which is dynamically coupled to the elevator motion and further to the rigid-body states. Finally, the operational condition varies drastically during flight, which leads to significant uncertainties in system dynamics. As an example, the speed of X-43A can change from Mach 7 to Mach 10, which results in a change of airframe and engine dynamics. These arguments render the hypersonic vehicle one of the most difficult plants for modeling and control.

Modeling of the dynamics of hypersonic vehicles has been addressed from various perspectives. Schmidt and Chavez provided a generic hypersonic vehicle model [1], [2]. In their model, an expression of the pressure acting on the vehicle was directly determined using Newtonian impact theory. This model was extended by Bolender and Doman [3], in which compressible flow theory was used to determine aerodynamic and propulsive forces, and Lagrange's method is invoked to derive the equations of motion for a flexible hypersonic vehicle. The advantage of this model is that the rigid-body motion and the flexible motion are combined in one set of equations. Hence, one can relatively easily see the dynamics of the rigid body and the elastic motion and how these two influence each other.

We propose a modified model in this paper to study the coupling dynamics between the flexible body and the rigid tail elevator. In the proposed model, the elevator is hinged at the end of the flexible aft-fuselage. The deflection of the elevator is calculated with respect to a fixed line of the rigid mid-fuselage. Since the rotation of the vehicle and bending of the flexible body will alter the orientation and position of the elevator, the pitch moment may depend on rate and acceleration, as well as the deflection of the control surface.

The rest of the paper is organized as follows. Section II develops the coupled model of the vehicle. In Section III, a brief introduction to the $\mathcal{L}_1$ adaptive controller is given. Control design for the vehicle is presented in Section IV. In Section V simulation results are presented.

II. Dynamical Model of Hypersonic Vehicle

The geometry of the notional model used is shown in Fig. II. The mid-fuselage is assumed to be a rigid-body. The aft-fuselage is assumed to be linearly elastic, and a is the distance from mid-fuselage mass center to the connecting point with the flexible beam. The relaxed length of the beam is l. A rigid elevator is connected to the other end of the flexible beam. The offset from the tail center of rotation to the mass-center of the elevator is denoted by d (positive if the center of mass is aft of the center of rotation), $\{\hat{e}_1, \hat{e}_2\}$ denotes the inertial frame, where $\hat{e}_1$ is the horizontal and $\hat{e}_2$ is the vertical component. The origin of the body frame is fixed at the mass center of the rigid mid-fuselage; $\hat{b}_1$ points backward along the unbending aft-fuselage and $\hat{b}_2$ is perpendicular to $\hat{b}_1$ and downward.

Research is supported by AFOSR under Contracts FA9550-07-1-0273, FA9550-08-1-0135 and by NASA under contracts NNX08BA65A and NNX08BA64A.

Y. Lei is with Virginia Tech, Blacksburg, VA; leiy@vt.edu, C. Cao is with UConn, Storrs, CT, N. Hovakimyan is with UIUC, IL, A. Kurdila is with Virginia Tech, Blacksburg, VA, E. Cliff is with Virginia Tech, Blacksburg, VA, K. Wise is with The Boeing Co., St. Louis, MO

978-1-4244-4524-0/09/$25.00 ©2009 AACC

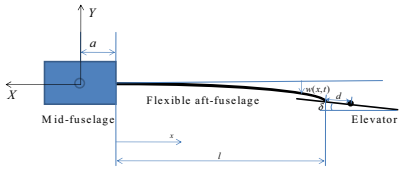

Fig. 1. Notional Model

The configuration of the system is determined by a set of variables $\{X(t), Y(t), \theta(t), \delta_e(t), w(x,t)\}$, where $(X(t), Y(t))$ is the position of the center of mass of the mid-fuselage, $\theta(t)$ is the pitch angle, $\delta_e(t)$ is the elevator deflection and $w(x,t)$ is the beam bending (x is measured along the body $\hat{b}_1$ axis), which is approximated using Ritz-Galerkin method, i.e. $w(x,t) = \boldsymbol{\varphi}^T(x)\boldsymbol{\xi}(t)$, where $\boldsymbol{\varphi}(x)$ is a vector of shape functions, and $\boldsymbol{\xi}(t)$ is the vibration state associated with $\boldsymbol{\varphi}(x) = [\varphi_1(x), \varphi_2(x), \ldots, \varphi_n(x)]^\top$, $\varphi_i(x) = -\frac{\cosh\beta_i l + \cos\beta_i l}{\sinh\beta_i l + \sin\beta_i l}(\sinh\beta_i x - \sin\beta_i x) + \cosh\beta_i x - \cos\beta_i x$ where β_i are roots of the equation $\cosh\beta_i l \cos\beta_i l + 1 = 0$. We use Hamilton's principle to derive the equations of motion, which states that for the actual path of motion the equation holds

$$\int_0^T \delta L dt + \int_0^T \delta W_{nc} dt = 0\,, \tag{1}$$

where $L = K - \Pi$ is the Lagrangian, and W_{nc} is the virtual work contributed by nonconservative forces. To compute the Lagrangian we express the body frame position and velocity components in the inertial frame. For the position vectors of the center of mass of the mid fuselage, of a generic point on the flexible aft fuselage and of the elevator's center of mass we have respectively ${}^E\mathbf{r}^m = X(t)\hat{e}_1 + Y(t)\hat{e}_2$, ${}^E\mathbf{r}^p = \hat{e}_1 X(t) + \hat{e}_2 Y(t) + (a+x)\hat{b}_1(t) + w(x,t)\hat{b}_2(t)$, ${}^E\mathbf{r}^t = \hat{e}_1 X(t) + \hat{e}_2 Y(t) + (a + l + d\cos\delta)\hat{b}_1(t) + (d\sin\delta + w(l,t))\hat{b}_2(t)$. Therefore, the kinetic energy K of the system can be computed as $K = \frac{1}{2}I_0\dot{\theta}^2 + \frac{1}{2}m_0\left({}^E\dot{\mathbf{r}}^m \cdot {}^E\dot{\mathbf{r}}^m\right) + \frac{1}{2}I_t(\dot{\delta}+\dot{\theta})^2 + \frac{1}{2}m_t\left({}^E\dot{\mathbf{r}}^t \cdot {}^E\dot{\mathbf{r}}^t\right) + \frac{1}{2}\int_0^l \sigma\, {}^E\dot{\mathbf{r}}^p \cdot {}^E\dot{\mathbf{r}}^p dx$, where m_0, I_0 and m_t, I_t are the mass and the moment of inertia of the mid-fuselage and the elevator respectively. The potential energy of the flexible aft fuselage can be computed as $\Pi = \frac{1}{2}\int_0^l EI w_{xx}^2 dx dx$, where E is the Young's modulus, and I is the moment of inertia of the cross section. The potential energy of the elevator due to gravity is ignored, as its mass is small compared to that of the mid-fuselage and flexible aft-fuselage.

There are five types of generalized nonconservative forces considered in the model: aero-dynamic forces acting on the elevator, the thrust, the actuator moment applied at the hinge point between the flexible body and the elevator, weight and damping force in flexible body. Variations of the virtual work corresponding to these forces are computed below. For the virtual work contributed by aero-dynamic forces we have $\delta W_{aero} = F \cdot \delta^E\mathbf{r}^m + M\delta\theta = (F_{2,c}\sin\theta - F_{1,c}\cos\theta)\,\delta X + (-F_{2,c}\cos\theta - F_{1,c}\sin\theta)\,\delta Y$, where $F = F_{1,c}\hat{b}_1 + F_{2,c}\hat{b}_2, F_{1,c} = D\cos\alpha - L\sin\alpha, F_{2,c} = -L\cos\alpha - D\sin\alpha, D = \frac{1}{2}\rho V_t^2 S_e C_D, L = \frac{1}{2}\rho V_t^2 S_e C_L, M = \frac{1}{2}\rho V_t^2 S_e \bar{c} C_M$. Here $F_{1,c}$ and $F_{2,c}$ are the resultant forces along $\{\hat{b}_1, \hat{b}_2\}$, while S_e is the area of the control surface. Aerodynamic forces are assumed to be acting at the C.G. of the mid-fuselage. Assuming that the thrust $\mathbf{T}$ is applied only to the rigid-body (the mid-fuselage), we can write $\mathbf{T} = \mathbf{T}(\cos\theta\hat{\mathbf{e}}_1 + \sin\theta\hat{\mathbf{e}}_2), \delta\mathbf{W}_\mathbf{T} = \mathbf{T}\cdot\delta\mathbf{r}^\mathbf{m} = \mathbf{T}\cos\theta\delta\mathbf{X} + \mathbf{T}\sin\theta\delta\mathbf{Y}$. The variation of the virtual work contributed by the actuator moment M_a applied at the hinge point has the form $\delta W_{M_a} = M_a\delta(\theta+\delta_e) - M_a\delta(\theta + w_x) = M_a\delta\delta_e - M_a\delta w_x(l,t)$.

It is assumed that the mass of the elevator is very small compared to that of the mid-fuselage and the flexible aft-body. Therefore, the contribution of gravity has the form $\delta W_g = \delta W_{\text{mid-fuselage}} + \delta W_{\text{flexible}} = g\sigma(al\cos\theta + \int_0^l x\cos\theta\,dx + \int_0^l \sin\theta w\,dx)\delta\theta - m_o g\delta Y - \sigma l g\delta Y + \int_0^l \sigma g\cos\theta\delta w\,dx$. Finally, damping is assumed to be mass-proportional (damping coefficient c is constant). $\delta W_{damping} = \int_0^l -c\dot{w}(x,t)\delta w\,dx$. The variation of the total virtual work of non-conservative forces can be expressed as the following sum: $\delta W_{nc} = \delta W_{aero} + \delta W_{M_l} + \delta W_T + \delta W_g + \delta W_{damping}$. Solving Eqn. (1) and applying the transformation $\dot{X} = V_t\cos\gamma$, $\dot{Y} = V_t\sin\gamma$, $\ddot{X} = \dot{V}_t\cos\gamma - V_t\dot{\gamma}\sin\gamma$, $\ddot{Y} = \dot{V}_t\sin\gamma + V_t\dot{\gamma}\cos\gamma$, we obtain the equations of motion in combined wind-body frame as follows $H(\mathbf{x})\dot{\mathbf{q}} + \mathbf{f}_1(\mathbf{x}) + \mathbf{f}_2(\mathbf{x}) + G(\mathbf{x})\mathbf{u} = \mathbf{0}$, where $\mathbf{x} = [h, V_t, \gamma, \theta, \dot{\theta}, \delta_e, \dot{\delta}_e, \boldsymbol{\xi}^\top, \dot{\boldsymbol{\xi}}^\top]^\top$ is the state vector, $\mathbf{q} = [V_t, \gamma, \dot{\theta}, \dot{\delta}_e, \dot{\boldsymbol{\xi}}^\top]^\top$ is the truncated state, $\mathbf{u} = [T, M_a]^\top$ is the control input, V_t is the vehicle speed and γ is the flight path angle. The matrices $H(\mathbf{x})$, $G(\mathbf{x})$ and the vector-functions $\mathbf{f_1}(\mathbf{x}), \mathbf{f_2}(\mathbf{x})$ have the form

$$G(\mathbf{x}) = \begin{bmatrix} \cos\alpha & 0 \\ \sin\alpha & 0 \\ 0 & 0 \\ 0 & 1 \\ \mathbf{0} & -\boldsymbol{\varphi}'(l) \end{bmatrix}$$

$$\mathbf{f}_1(\mathbf{x}) = \begin{bmatrix} c_1\cos(\alpha)\dot{\theta} - a_2\dot{\theta}^2 - dm_t\cos(\delta_e+\alpha)(\dot{\delta}_e+\dot{\theta})^2 \\ c_1\sin(\alpha)\dot{\theta} + a_1\dot{\theta}^2 - dm_t\sin(\delta_e+\alpha)(\dot{\delta}_e+\dot{\theta})^2 \\ c_2\dot{\theta} + a_4\dot{\delta}^2 + 2a_4\dot{\theta}\dot{\delta} \\ -2dm_t\sin(\delta)\boldsymbol{\varphi}^\top(l)\dot{\boldsymbol{\xi}}\dot{\theta} + a_4\dot{\theta}^2 \\ a_8\dot{\theta}^2\boldsymbol{\xi}(t) + \boldsymbol{\varphi}(l)dm_t\sin\delta_e(\dot{\delta}_e+\dot{\theta})^2 - c\mathbf{b}_1\dot{\boldsymbol{\xi}} \end{bmatrix}$$

$$\mathbf{f}_2(\mathbf{x}) = \begin{bmatrix} -D - g(m_0 + l\sigma)\sin\gamma \\ L - g(m_0+l\sigma)\cos\gamma \\ (agl\sigma + \frac{1}{2}\sigma g l^2)\cos\theta + (\sigma g\boldsymbol{\varphi}_1^\top\boldsymbol{\xi})\sin\theta + M \\ 0 \\ +\sigma\mathbf{b}_1 g\cos\theta - EIK_3\boldsymbol{\xi} \end{bmatrix}$$

$$H(\mathbf{x}) = \begin{bmatrix} -m & 0 & a_1 & -dm_t\sin(\delta_e+\alpha) & -(\boldsymbol{\varphi}^\top(l)m_t + \mathbf{b}_1^\top\sigma)\sin\alpha \\ 0 & -mV_t & a_2 & dm_t\cos(\delta_e+\alpha) & (\boldsymbol{\varphi}^\top(l)m_t + \mathbf{b}_1^\top\sigma)\cos\alpha \\ a_1 & V_t a_2 & a_6 & -I_t - d^2m_t - a_3 & \mathbf{b}_3^\top \\ -dm_t\sin(\alpha+\delta_e) & dm_t\cos(\delta_e+\alpha)V_t & a_7 & -I_t - d^2m_t & -\boldsymbol{\varphi}^\top(l)dm_t\cos\delta_e \\ -\mathbf{b_4}\sin\alpha & \mathbf{b_4}V_t\cos(\alpha) & \mathbf{b}_5 & -\boldsymbol{\varphi}(l)dm_t\cos\delta_e & -(\sigma K_1 + K_2) \end{bmatrix} \tag{2}$$

Please refer to the Appendix for the definition of the terms.

A. Control Objective

The state of the system is $\mathbf{x} = [h, V_t, \gamma, \theta, \dot{\theta}, \xi, \dot{\xi}]^T$, in which $h, V_t, \gamma, \theta, \dot{\theta}, \xi, \dot{\xi}$ are the vehicle altitude, the vehicle speed, flight path angle, pitch angle, pitch rate, vibration mode and its time derivative, respectively. The control input of the system is $u = [T, \delta_e]$, where δ_e is the elevator deflection and T is the thrust. We assume that $h, V_t, \gamma, \theta, \dot{\theta}$ can be measured by available sensors. The control objective is to ensure that the vehicle's velocity V_t and the flight path angle γ follow the given reference signals, while all other variables remain bounded.

III. Introduction to $\mathcal{L}_1$ Adaptive Controller

In this section, we will give a brief introduction to $\mathcal{L}_1$ adaptive controller, [13]. Consider the following general form of the system dynamics:

$$\begin{aligned} \dot{x}(t) &= A_m x(t) + b(\mu(t) + f(x(t), z(t), t)) \\ \dot{z}(t) &= g(x(t), z(t), u(t), t) \\ \mu(s) &= F(s)u(s) \\ y(t) &= c^\top x(t), \qquad x(0) = x_0, \end{aligned} \tag{3}$$

where $x \in \mathbb{R}^n$ is the system state vector (measurable), $u \in \mathbb{R}$ is the control signal, $y \in \mathbb{R}$ is the regulated output, $b, c \in \mathbb{R}^n$ are known constant vectors, A_m is a known $n \times n$ Hurwitz matrix, z is the state vector of the bounded-input bounded-output (BIBO) stable unmodeled dynamics, $F(s)$ is an unknown stable transfer function, while f, g are unknown nonlinear functions.

Assumption 1: There exist bounded L_1 and L_2 such that $\|f(x(t), z(t), t)\| \leq L_1 \|x(t)\|_\infty + L_2$.

Assumption 2: The partial derivatives of $f(x, z, t)$ are piece-wise continuous and bounded.

Assumption 3: There exists L_F such that $\|F(s)\|_{\mathcal{L}_1} \leq L_F$, where $\|F(s)\|_{\mathcal{L}_1}$ denotes the $\mathcal{L}_1$-norm of the system.

It follows from Assumptions 1 and 2 that there exist bounded $\theta(t)$ and $\sigma(t)$ such that $f(x(t), z(t), t) = \theta(t)\|x(t)\|_\infty + \sigma(t)$, where the unknown time-varying parameters and the disturbances are uniformly bounded:

$$|\theta(t)| \leq L_1, \quad |\sigma(t)| \leq L_2 , \quad \forall\, t \geq 0 , \tag{4}$$

and continuously differentiable with uniformly bounded derivatives:

$$|\dot{\theta}(t)| \leq d_\theta < \infty, \quad |\dot{\sigma}(t)| \leq d_\sigma < \infty, \quad \forall\, t \geq 0 . \tag{5}$$

The design of $\mathcal{L}_1$ adaptive controller involves a feedback gain $k \in \mathbb{R}^+$ and a strictly proper transfer function $D(s) = \frac{1}{s}\bar{D}(s)$, where $\bar{D}(s)$ is proper and stable, which leads to a strictly proper stable

$$C(s) = \frac{kF(s)D(s)}{1 + kF(s)D(s)} \tag{6}$$

with DC gain $C(0) = 1$. The simplest choice of $D(s)$ is $D(s) = 1/s$ $(\bar{D}(s) = 1)$. Let $r_0(t)$ be the signal with its Laplace transform $(s\mathbb{I} - A_m)^{-1}x_0$. Since A_m is Hurwitz and x_0 is finite, $\|r_0\|_{\mathcal{L}_\infty}$ is finite. Further, let

$$\begin{aligned} \rho_r &= \Big(\|\bar{G}(s)\|_{\mathcal{L}_1}\|L_2 + \|H(s)C(s)k_g\|_{\mathcal{L}_1}\|r\|_{\mathcal{L}_\infty} \\ &\quad + \|r_0\|_{\mathcal{L}_\infty}\Big)/(1 - \|\bar{G}(s)\|_{\mathcal{L}_1}L_1) , \\ \rho_{u_r} &= \Big\|\frac{kD(s)}{1 + kD(s)F(s)}\Big\|_{\mathcal{L}_1}(L_1\rho_r + L_2 + k_g\|r\|_{\mathcal{L}_\infty}), \end{aligned} \tag{7}$$

where $k_g = -1/(c^\top A_m^{-1} b)$, and $\bar{G}(s) = H(s)(1 - C(s))$, $H(s) = (s\mathbb{I} - A_m)^{-1}b$. Finally, let $\rho_u = \rho_{u_r} + \gamma$, where γ is an arbitrary positive constant. The elements of $\mathcal{L}_1$ adaptive controller are introduced next:

State Predictor: We consider the following state predictor:

$$\begin{aligned} \dot{\hat{x}}(t) &= A_m\hat{x}(t) + b\Big(\hat{\omega}(t)u(t) + \hat{\theta}(t)\|x(t)\|_\infty + \hat{\sigma}(t)\Big) , \\ \hat{y}(t) &= c^\top\hat{x}(t) , \quad \hat{x}(0) = x_0 , \end{aligned} \tag{8}$$

where the adaptive estimates $\hat{\omega}(t), \hat{\theta}(t), \hat{\sigma}(t)$ are governed by the following adaptation laws.

Adaptive Laws: Adaptive estimates are given by:

$$\begin{aligned} \dot{\hat{\theta}}(t) &= \Gamma_\theta \mathrm{Proj}(\hat{\theta}(t), -\tilde{x}^\top(t)Pb\|x(t)\|_\infty), \qquad \hat{\theta}(0) = \hat{\theta}_0 \\ \dot{\hat{\sigma}}(t) &= \Gamma_\sigma \mathrm{Proj}(\hat{\sigma}(t), -\tilde{x}^\top(t)Pb), \qquad \hat{\sigma}(0) = \hat{\sigma}_0 \\ \dot{\hat{\omega}}(t) &= \Gamma_\omega \mathrm{Proj}(\hat{\omega}(t), -\tilde{x}^\top(t)Pbu(t)), \qquad \hat{\omega}(0) = \hat{\omega}_0 , \end{aligned} \tag{9}$$

where $\tilde{x}(t) = \hat{x}(t) - x(t)$ is the error signal between the states of the system and the predictor, $\Gamma \in \mathbb{R}^+$ is the adaptation gain, P is the solution of the algebraic equation $A_m^\top P + PA_m = -Q$, $Q > 0$, and the projection operator ensures that the adaptive estimates $\hat{\omega}(t)$, $\hat{\sigma}(t)$ remain inside the compact sets $[\omega_l,\ \omega_h]$, $[-\sigma_b,\ \sigma_b]$, respectively, where ω_l and ω_h are chosen to be nonzero constants with the same sign, and σ_b is the following upper bound: $\sigma_b > L_2 + \|F(s) - (\omega_l + \omega_h)/2\|_{\mathcal{L}_1}\rho_u$, and $\hat{\theta}(t)$ remains bounded according to (4), i.e. $|\hat{\theta}(t)| \leq L_1$.

Control Law: The control signal is generated through feedback of the following system:

$$\chi(s) = D(s)\bar{r}(s), \quad u(s) = -k\chi(s) , \tag{10}$$

where $\bar{r}(s)$ is the Laplace transform of $\bar{r}(t) = \hat{\omega}(t)u(t) + \hat{\theta}(t)\|x(t)\|_\infty + \hat{\sigma}(t) - k_g r(t)$. The stability and performance bounds of $\mathcal{L}_1$ adaptive controller given by (8), (9) and (10) are proven in [13] in the presence of the following $\mathcal{L}_1$-norm upper bound: $\|\bar{G}(s)\|_{\mathcal{L}_1}L_1 < 1$.

IV. Controller Design

The analysis of the linearized hypersonic model (in the coming subsection) shows that this system has several modes with quite different time constants. The phugoid mode has the time constant about hundreds of seconds, while the short period mode may reach its steady state within a couple of seconds. The fundamental frequency of fuselage vibration is about $2Hz$. We will divide the system into several loops according to their different time constants and stabilize each

loop in the presence of unmodeled dynamics. The inner-loop stabilization would be a pitch axis stability augmentation system. The virtual control for this loop is the elevator deflection δ_e. The control objective of this loop is to stabilize the short-period modes and leave the long period modes unaltered. Since the hypersonic flights are at very high speed, there is significant vibration/disturbance between the torque driving the elevator and the actual deflection of the elevator. If we regard the virtual control δ_e calculated in the previous step as a "reference signal" δ_{ec}, the difference between the actual deflection δ_e and the preferred value δ_{ec} due to vibration/disturbance can be viewed as unmodeled actuator dynamics. The $\mathcal{L}_1$ adaptive control architecture is used to address this challenge. The controller should be able to maintain the vehicle pitch angle θ in the presence of unmodeled disturbances. Then, the outer-loop controller is used to change the speed to its desired value by providing appropriate thrust. Finally, the altitude control is attained by maintaining the speed of hypersonic vehicle and generating appropriate command signal of flight path angle γ_{com}.

A. Analysis of the Linearized Model

Before we go ahead with the controller design, we study the linearized model. Readers are referred to the Appendix for the geometry and physical data of the model. For simplicity we only expand the shape function of the flexible fuselage at its first mode, i.e. we consider $\boldsymbol{\phi}(x) = \phi_1(x)$ with $\beta_1 = 1.875/l$. It is assumed that the vehicle speed V_t, the flight path angle γ, the pitch angle θ, the elevator deflection δ_e and the generalized vibration modes ξ all remain constant at the trimmed point. In other words, the trimmed point $\mathbf{x}^*$ is a solution of $\boldsymbol{f}_2(\mathbf{x}^*) + G(\mathbf{x}^*)\mathbf{u}^* = 0$. Numerical result for the trimmed condition of level flight at the speed of 2380 $\mathrm{m/s}$ (Mach 8 at 85,000 ft) is $V_t = 2380\mathrm{m/s},\ \gamma = 0, \theta = 1.62\mathrm{deg},\ \delta_e = 11.4\mathrm{deg},\ \xi = 0.04\mathrm{m},\ T = 1.12 \times 10^4\mathrm{N}$. The following linearized model at the operation point $\dot{x} = Ax + Bu$ is obtained with A and B given in Appendix. The state variables can be further divided into three categories: $\mathbf{x}_{rigid} = [V_t, \gamma, \theta, q]^\top$ can be referred to as rigid body state and the virtual control for this sub-system is the elevator deflection δ_e. Next, $\mathbf{x}_{act} = [\delta_e, \dot{\delta}_e]^\top$ describes the dynamics of the servo motor, which drives the elevator. The vibration states, which are not directly measured by the sensors, are $\mathbf{x}_{flex} = [\xi, \dot{\xi}]^\top$. The linearized dynamics can therefore be rewritten as:

$$\begin{aligned}\dot{\mathbf{x}} &= \begin{pmatrix} A_{rigid} & B_{\delta_e} & 0 & B_{flex1} \\ B_{rigid1} & A_{act} & & B_{flex2} \\ B_{rigid2} & B_{act} & & A_{flex} \end{pmatrix}\mathbf{x} + \begin{pmatrix} B_1 \\ B_2 \\ B_3 \end{pmatrix}\mathbf{u} \\ \mathbf{x} &= [\mathbf{x}_{rigid}, \mathbf{x}_{act}, \mathbf{x}_{flex}]^\top\end{aligned}$$

Next we discuss each subsystem in details.

1) Rigid-Body Subsystem: The dynamics of the rigid body are given by $\dot{\mathbf{x}}_{rigid} = A_{rigid}\mathbf{x}_{rigid} + B_1\delta_e + B_1\mathbf{u} + B_{flex1}\mathbf{x}_{flex}$. Eigenvalues of this subsystem are $-0.0007 \pm 0.0073i, 6.7883, -6.8911$. The pair of the complex poles is the long period mode (open-loop vehicle speed V_t has a damping ratio of $\zeta = 0.09$ and a time constant of about 850 sec). The two real poles are those of the short-period dynamics and are not stable. From the equation one can also find that the speed is dominantly influenced by thrust T, which however has very limited effect on pitch loop states, i.e. flight path angle γ, pitch angle θ and pitch rate $\dot{\theta}(q)$. Due to hypersonic vehicle's high velocity and its slender structure, rigid-body variables are heavily disturbed by flexible body vibrations. It can also be found from the linear equation that the control torque M_a does not directly change the states of the rigid-body, but through servo dynamics. An immediate analysis shows that not only δ_e, but also its higher order derivatives are coupled with rigid-body states.

From the above discussion one can find that the vehicle's speed V_t does not change rapidly as compared to γ, θ, q, therefore $\dot{V}_t$ is assumed to be trivial in the following analysis. Letting $\mathbf{x}_p = [\gamma, \theta, q]^\top$, the nonlinear dynamics for $\mathbf{x}_p$ are given by $E(\mathbf{x})\dot{\mathbf{x}}_p = F(\mathbf{x})$. When $\mathbf{x}_p$ and δ_e are near to their trimmed values $\mathbf{x}_p^*$ and δ_e^*, it can be approximated as:

$$E\delta\dot{\mathbf{x}}_p = \frac{\partial F}{\partial \mathbf{x}_p}\delta\mathbf{x}_p + \frac{\partial F}{\partial \delta_e}\delta\delta_e + \frac{\partial F}{\partial \ddot{\delta}_e}\delta\ddot{\delta}_e + \frac{\partial F}{\partial \ddot{\xi}}\delta\ddot{\xi}, \qquad (11)$$

where $E = \begin{pmatrix} -mV_t^* & 0 & a_2 \\ 0 & 1 & 0 \\ V_t^* a_2 & 0 & a_6 \end{pmatrix}$, $\frac{\partial F}{\partial x} = -\begin{pmatrix} -L_{,\alpha} - T^* & +L_{,\alpha} + T^* & 0 \\ 0 & 0 & -1 \\ -M_{,\alpha} & M_{,\alpha} + \sigma g\phi\xi^* & 0 \end{pmatrix}$, $\frac{\partial F}{\partial \delta_e} = -\begin{pmatrix} C_{L,\delta_e} \\ 0 \\ C_{M,\delta} \end{pmatrix}$, $\frac{\partial F}{\partial \ddot{\delta}_e} = -\begin{pmatrix} 0 \\ 0 \\ I_t \end{pmatrix}$, $\frac{\partial F}{\partial \ddot{\xi}} = -\begin{pmatrix} W_1 \\ 0 \\ W_2 \end{pmatrix}$, $W_1 = -(\boldsymbol{\varphi}^\top(l)m_t + \mathbf{b}_1^\top\sigma)\sin\alpha$, $W_2 = -(\boldsymbol{\varphi}^\top(l)m_t + \mathbf{b}_1^\top\sigma)\cos\alpha$, $m = m_0 + m_t + \sigma l$, where a_2, a_6 are given in Appendix and will be treated as constants. Further, $L_{,\alpha}$ is the partial derivative of L with respect to α, $L_{,\delta}, D_{,\alpha}, M_{,\alpha}$ are defined similarly, i.e. $L_{,\alpha} = \frac{\partial L}{\partial \alpha} = \frac{1}{2}\rho V_t^2 S_e \frac{\partial C_L}{\partial \alpha}, D_{,\alpha} = \frac{\partial D}{\partial \alpha} = \frac{1}{2}\rho V_t^2 S_e \frac{\partial C_D}{\partial \alpha}, M_{,\alpha} = \frac{\partial M}{\partial \alpha} = \frac{1}{2}\rho V_t^2 S_e \bar{c}^2 \frac{\partial C_M}{\partial \alpha}$. It is clear from Eqn. (11) that the rigid-body motion depends not only on elevator deflection δ_e, but also on its derivative $\ddot{\delta}_e$ and the derivative of elastic modes $\ddot{\xi}$. Another obvious observation is that $W_2 \gg W_1$, which implies that the vibration is mainly coupled with pitch rate q and its direct effect on flight path angle γ is negligible.

2) Actuator Subsystem: The angular position of the elevator is driven by a motor, and the linear equation of motion for the dynamics is $\dot{\mathbf{x}}_{act} = A_{act}\mathbf{x}_{act} + B_2 M_a + B_{rigid1}\mathbf{x}_{rigid} + B_{flex2}\mathbf{x}_{flex}$. The open-loop eigenvalues of the subsystem are ± 3.0971. In order to follow a given reference signal $\delta_{e\,ref}$, an adaptive controller has to be designed to stabilize the subsystem with very quick response time in the presence of disturbance.

3) Flexible Fuselage subsystem: The numerical data of the subsystem $\dot{\mathbf{x}}_{flex} = A_{flex}\mathbf{x}_{flex} + B_{rigid2}\mathbf{x}_{rigid} + B_{act}\mathbf{x}_{act} + B_3 M_a$ show that flexible fuselage motion can be treated as a 1-DOF vibration excited by the rigid-body variables θ, γ, δ_e and the control M_a. The frequency and damping ratio are $\omega_d = 1.9\mathrm{Hz}$ and $\zeta = 0.013$, respectively.

B. $\mathcal{L}_1$ Controller for Pitch Axis Stability Augmentation

As stated above, a stability augmentation system (SAS) is required since one pole of the short-period mode is not stable. The main function of the adaptive controller $\delta_{e\,com} = u_{apt}(\theta, q, \gamma, \theta_{com})$ is to hold the pitch angle θ at its preferred position θ_{com}, with settling time about 10 seconds. One of the two design challenges in this subsystem is the unmodeled dynamics in the actuator $\delta_e/\delta_{e\,com}$. The other one is that the vibration from the flexible part is heavily coupled with the vehicle's pitch rate. The variables involved in the SAS are V_t, γ, θ, q and δ_e, which are treated as virtual control inputs. The state equation of the system is given by $\dot{x}_{sas} = A_{sas}x + B_{sas}\delta_e$. The system is considered as a cascaded system, where pitch-loop (θ, q) is treated as the inner-loop since it has a faster time constant and speed V_t and path-angle γ belong to the outer-loop.

The parameters of the controller for the pitch-loop are $A_m = [0\ 1; -400\ -40], b = [0; -11], \Gamma_\theta = 30000, \Gamma_\sigma = 30000, \Gamma_\omega = 30000, D(s) = \frac{1}{s}$, $k = 20, Q = \mathbb{I}_{2\times 2}$.

C. $\mathcal{L}_1$ Controller for Outer-loop (flight path angle γ)

The parameters for this loop are $A_m = -0.06\,, b = 0.06$, $\Gamma_\theta = 5000, \Gamma_\sigma = 5000, \Gamma_\omega = 5000, D(s) = \frac{0.12}{s+0.12}$, $k = 1, Q = 1$.

D. $\mathcal{L}_1$ Controller for Outer-loop (Velocity V_t)

The parameters for this loop are $A_m = -0.02\,, b = 0.02$, $\Gamma_\theta = 1000, \Gamma_\sigma = 1000, \Gamma_\omega = 1000, D(s) = \frac{1}{s}$, $k = 20, Q = 1$.

E. $\mathcal{L}_1$ Controller for Altitude h

The parameters for this loop are $A_m = -0.025\,, b = 0.025$, $\Gamma_\theta = 2000, \Gamma_\sigma = 2000, \Gamma_\omega = 2000, D(s) = \frac{0.1}{s+0.1}$, $k = 10, Q = 1$.

V. Simulation

The simulations are done with a mid-fuselage mass 2800 kg and flexible body mass 1600 kg, $EI = 1.9 \times 10^6 \mathrm{N} \cdot \mathrm{m}^2$, $a = 2m$ and $l = 10m$. We prepared three scenarios to test the pitch-loop controller, the velocity loop controller and the altitude controller respectively. Note that the inner-pitch-loop is exercised in all these tests. Since the vehicle is a nonlinear open-loop unstable plant, it has to be under the $\mathcal{L}_1$ controller continuously to be able to operate at its trimmed condition until the 50th second, when there will be a change of a certain command. Simulation results of the first test are given in Fig. 2, where the flight path angle was at rest of 0 degree. At the 50th second the command reference steps to 3 degree. One could tell from the simulation result that the response time of the flight path angle γ is about 170 seconds. As discussed before, the vehicle vibrates due to its slender flexible structure and control δ_e oscillates as well trying to cancel the flexible fuselage's effect on the system output Fig. 2(b). Simulation results (zoomed-in part in Fig. 2(a)) show that the oscillations' effect on the vehicle's flight path angle was suppressed to a very low amplitude. One can also see from Fig. 2(c) that the vehicle speed decreases, when the flight path angle is increased. The engine also has to generate more power, when we increase the vehicle's flight path angle and maintain its speed.

The test results for the velocity controller are shown in Fig. 3. The initial velocity of the second simulation test is 2400 $\mathrm{m/s}$ until the 50th second ,when it changes the speed up to 2500 $\mathrm{m/s}$. The response time of the velocity is about 200 seconds. Similar to the situation in the first test, changing of vehicle speed also disturbs the flight path angle, but the controller can easily recover the vehicle's level flight condition.

The behavior of the altitude controller is demonstrated in Fig.4. In the beginning, the vehicle was making a level flight at 85000 ft and at the 50th second, it tries to climb up to 88000 ft. From the simulation result, it takes the vehicle about 200 seconds to fulfill the task.

VI. Conclusions

A new mathematical model for an air-breathing hypersonic vehicle model is proposed and a novel $\mathcal{L}_1$ adaptive controller for the vehicle model is presented. The model shows that there is heavy dynamic coupling between fuselage bending and elevator deflection. Simulation data show the vibration in the pitch loop from dynamic coupling was suppressed by the $\mathcal{L}_1$ adaptive controller.

References

[1] F. R. Chavez and D. K. Schmidt, Analytical aeropropulsive-aeroelastic hypersonic-vehicle model with dynamic analysis, Journal of Guidance, Control, and Dynamics, vol.17, No.6, pp.1308-1319, 1994

[2] D. Sigthorsson, A. Serrani, S. Yurkovich, M. Bolender and D. Doman, Tracking Control for an Overactuated Hypersonic Air-Breathing Vehicle with Steady State Constraints, AIAA Guidance, Navigation, and Control Conference and Exhibit, Keystone, Colorado, Aug. 21-24, 2006, AIAA-2006-6558.

[3] M. Bolender and D. Doman, A Non-Linear Model for the Longitudinal Dynamics of a Hypersonic Air-breathing Vehicle, AIAA Guidance, Navigation, and Control Conference and Exhibit, San Francisco, California, Aug. 15-18, 2005, AIAA-2005-6255.

[4] M. Bolender and D. Doman, Nonlinear Longitudinal Dynamical Model of an Air-Breathing Hypersonic Vehicle, Journal of Spacecraft And Rockets, Vol. 44, No. 2, March-April 2007

[5] H. Xu , M. D. Mirmirani and P. A. Ioannou, Adaptive Sliding Mode Control Design for a Hypersonic Flight Vehicle, Journal of Guidance, Control, and Dynamics, vol.27, no.5, pp.829-838, 2004.

[6] K. Groves, D. Sigthorsson, A. Serrani and S. Yurkovich, Reference Command Tracking for a Linearized Model of an Air-Breathing Hypersonic Vehicle, AIAA Guidance, Navigation, and Control Conference and Exhibit, San Francisco, California, Aug. 15-18, 2005, AIAA-2005-6144.

[7] J. T. Parker, A. Serrani and S. Yurkovich, Approximate Feedback Linearization of an Air-breathing Hypersonic Vehicle, AIAA Guidance, Navigation, and Control Conference and Exhibit, Keystone, Colorado, Aug. 21-24, 2006, AIAA 2006-6556.

[8] T. A. Adami, J. Zhu, M. Bolender and D. Doman, Flight Control of Hypersonic Scramjet Vehicls Using a Differential Algebraic Approach, AIAA Guidance, Navigation, and Control Conference and Exhibit, Keystone, Colorado, Aug. 21-24 2006.

[9] C. Cao and N. Hovakimyan, Design and Analysis of a Novel $\mathcal{L}_1$ Adaptive Control Architecture with Guaranteed Transient Performance, *IEEE Transactions on Automatic Control*, 53(2):586-891, 2008.

[10] C. Cao and N. Hovakimyan, Adaptive Output Feedback Controller for Systems of Unknown Dimension, *IEEE Transactions on Automatic Control*, 53(3):815-821, 2008.

[11] C. Cao and N. Hovakimyan. $\mathcal{L}_1$ adaptive controller for systems with unknown time-varying parameters and disturbances in the presence of non-zero trajectory initialization error. *International Journal of Control*, 81(7):1147–1161, 2008.

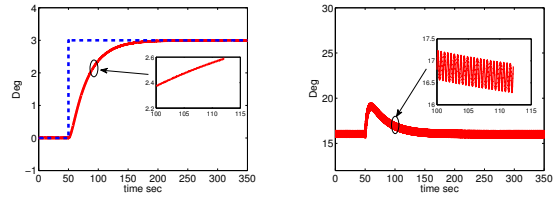

(a) flight path angle γ (b) elevator deflection δ_e

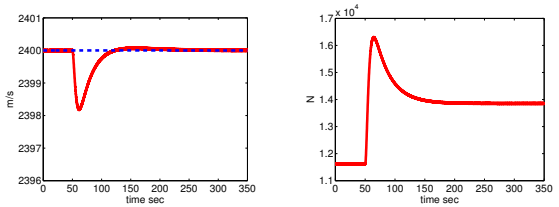

(c) speed V_t (d) thrust

Fig. 2. State/control responses to path-angle command (solid: system response dashed: command)

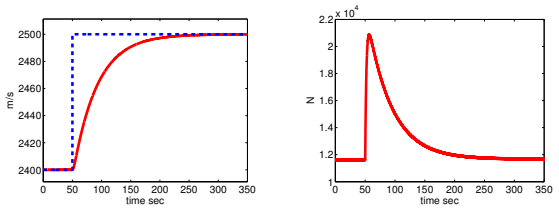

(a) speed V_t (b) thrust

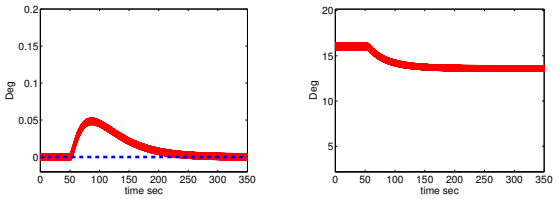

(c) flight path angle γ (d) elevator deflection δ_e

Fig. 3. State/control responses to speed command (solid: system response dashed: command)

[12] C. Cao and N. Hovakimyan,Stability Margins of $\mathcal{L}_1$ Adaptive Control Architecture, *American Control Conference*, pp. 3931-3936, 2007.

[13] C. Cao and N. Hovakimyan, $\mathcal{L}_1$ Adaptive Controller for Systems in the Presence of unmodeled Actuator Dynamics, IEEE Conference on Decision and Control, pp. 891-896, 2007.

VII. Appendix

The notations are $a_1 = -a_m \sin\alpha - (m_t w(l,t) + \sigma\boldsymbol{\xi}^T\mathbf{b_1})\cos\alpha, a_2 = a_m\cos\alpha - (m_t w(l,t) + \sigma\boldsymbol{\xi}^T\mathbf{b_1})\sin\alpha, a_m = \frac{\sigma l^2}{2} + m_t l + a\sigma l + am_t, a_3 = (a+l)m_t d\cos\delta + m_t d w(l,t)\sin\delta_e, a_4 = (a+l)m_t d\sin\delta - m_t d w(l,t)\cos\delta_e, a_5 = -\frac{\sigma}{3}\left((a+l)^3 - a^3\right) - m_t(l+a)^2 - d^2 m_t - I_0 - I_t, a_6 = a_5 - m_t w(l,t)^2 - 2a_3 - \boldsymbol{\xi}^T K_1\boldsymbol{\xi}, a_7 = -I_t - d^2 m_t - a_3, a_8 = \sigma K_1 + K_2, \mathbf{b}_1 = \int_0^l \boldsymbol{\varphi}(x)dx, \mathbf{b}_2 = \int_0^l \boldsymbol{\varphi}(x)xdx, \mathbf{b}_3 = -\boldsymbol{\varphi}(l)m_t(a + l + d\cos\delta) - a\mathbf{b}_1\sigma, \mathbf{b}_4 = \boldsymbol{\varphi}(l)m_t + \mathbf{b}_1\sigma, \mathbf{b}_5 = -\boldsymbol{\varphi}(l)m_t(a + l + d\cos\delta) - \sigma(a\mathbf{b}_1 + \mathbf{b}_2)\sigma, K_1 = \int_0^l \boldsymbol{\varphi}(x)\boldsymbol{\varphi}^\top(x)dx, K_2 = \boldsymbol{\varphi}(l)m_t\boldsymbol{\varphi}^\top(l), K_3 = \int_0^l \boldsymbol{\varphi}_{xx}(x)\boldsymbol{\varphi}_{xx}^\top(x)\,dx, c_1 = -2m_t\boldsymbol{\varphi}^\top(l)\dot{\boldsymbol{\xi}} - 2\mathbf{b}_1^\top\dot{\boldsymbol{\xi}}\sigma, c_2 = -2\boldsymbol{\varphi}(l)^\top\dot{\boldsymbol{\xi}}m_t(d\sin(\delta) + \boldsymbol{\varphi}^\top(l)\boldsymbol{\xi}) - 2\dot{\boldsymbol{\xi}}^\top K_1\boldsymbol{\xi}\sigma$. Also, $\varphi_i(x) = -\frac{\cosh\beta_i l + \cos\beta_i l}{\sinh\beta_i l + \sin\beta_i l}(\sinh\beta_i x - \sin\beta_i x) + \cosh\beta_i x - \cos\beta_i x$, $\cosh\beta_i l = -\frac{1}{\cos\beta_i l}, D = \frac{1}{2}\rho V_t^2 S_e C_D, L = \frac{1}{2}\rho V_t^2 S_e C_L, M = \frac{1}{2}\rho V_t^2 S_e\bar{c}C_M$ where m and m_t are mass of the rigid-fuselage and the elevator, respectively, σ is the linear density of the flexible aft-fuselage. The unbending length of the fuselage is l and shape of the aft-fuselage is $w(x,t) = \boldsymbol{\xi}^\top(t)\boldsymbol{\varphi}(x), x \in [0,l]$, a is the dimension of the rigid mid-fuselage and d is the distance between the hinge point and the mass center of the all-movable elevator, T is the thrust and D, L, M are the drag, lift and pitch moment of the hypersonic vehicle, respectively, S_e is the area of the control surface, and ρ is the density of atmosphere.

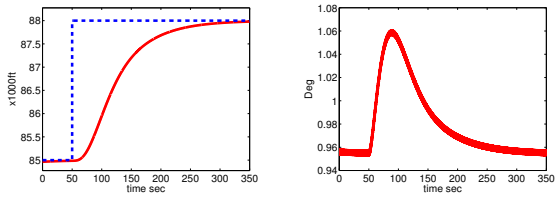

(a) altitude h (b) flight path angle γ

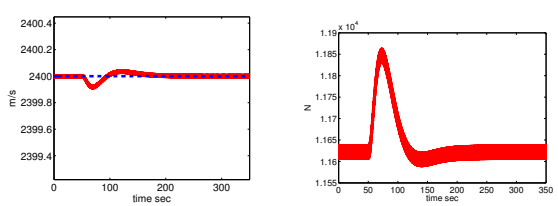

(c) speed V_t (d) thrust

Fig. 4. State/control responses to altitude command (solid: system response dashed: command)

$$A_{sas} = \begin{pmatrix} -0.0016 & 4.4895 & -14.219 & 0 \\ 0 & -0.2025 & 0.2025 & 0 \\ 0 & 0 & 0 & 1 \\ 0.0009 & -47.4562 & 47.4571 & 0 \end{pmatrix}$$

$$B = \begin{pmatrix} 0.0001 & 0 \\ -0 & -0 \\ 0 & 0 \\ -0 & -0 \\ 0 & 0 \\ 0 & 0.1607 \\ 0 & 0 \\ -0 & -0.0001 \end{pmatrix}, B_{sas} = \begin{pmatrix} 0.0126 \\ -0.0054 \\ 0 \\ -0.4315 \end{pmatrix}$$

$$A = \begin{pmatrix} -0.0016 & 4.4895 & -14.219 & 0 & -11.0521 \\ 0 & -0.2025 & 0.2025 & 0 & -0.009 \\ 0 & 0 & 0 & 1 & 0 \\ 0.0009 & -47.4562 & 47.4571 & 0 & -9.5514 \\ 0 & 0 & 0 & 0 & 0 \\ -0.0009 & 47.4562 & -47.4571 & 0 & 9.5514 \\ 0 & 0 & 0 & 0 & 0 \\ 0.0387 & -1507.2073 & 1507.2566 & 0 & -181.9497 \end{pmatrix}$$

$$\begin{pmatrix} 0 & 0.6006 & 0.0009 \\ 0 & -0.0107 & -0 \\ 0 & 0 & 0 \\ 0 & 1.7965 & 0.0023 \\ 1 & 0 & 0 \\ 0 & -1.7965 & -0.0023 \\ 0 & 0 & 1 \\ 0 & -236.3847 & -0.3005 \end{pmatrix}$$